DISCLAIMER

This report was prepared as an account of work sponsored by an agency of the United States Government. Neither the United States Government nor any agency thereof, nor any of their employees, makes any warranty, express or implied, or assumes any legal liability or responsibility for the accuracy, completeness, or usefulness of any information, apparatus, product, or process disclosed, or represents that its use would not infringe privately owned rights. Reference herein to any specific commercial product, process, or service by trade name, trademark, manufacturer, or otherwise does not necessarily constitute or imply its endorsement, recommendation, or favoring by the United States Government or any agency thereof. The views and opinions of authors expressed herein do not necessarily state or reflect those of the United States Government or any agency thereof.

ANL/RE/CP--85952
Conf-950740--64

The submitted manuscript has been authored by a contractor of the U. S. Government under contract No. W-31-109-ENG-38. Accordingly, the U. S. Government retains a nonexclusive, royalty-free license to publish or reproduce the published form of this contribution, or allow others to do so, for U. S. Government purposes.

SLOSHING IMPACT IN ROOFED TANKS

R. Aziz Uras
Reactor Engineering Division
Argonne National Laboratory
Argonne, Illinois

ABSTRACT

A large number of high-level waste (HLW) storage tanks exists in various tank farms. Seismic activities at those locations may cause significant sloshing in HLW tanks. These tanks are covered to avoid any spilling during large amplitude earthquakes. However, large amplitude sloshing may result in impact on the cover or the roof of the tank. Hence, a better understanding of the impact phenomenon is necessary to assess the safety of the tanks currently in existence, and to establish design guidelines for future designs. A pressure based formulation is derived to model sloshing impact in roofed tanks. It is incorporated into Argonne's in-house finite element code FLUSTR-ANL. A numerical test case with a harmonic input excitation is studied. The simulation results indicate that linear behavior is preserved beyond the first impact, and some mesh distortion is observed following a stronger second impact. During the impact, the displacement of the contacting surface nodes remains constant, and the velocities are reduced to zero. An identification of impacting nodes is possible from the dynamic pressures induced in surface elements.

INTRODUCTION

Due to the potential risk to the environment, the safety assessment of high-level waste (HLW) storage tanks is becoming an important issue. The currently accepted design guidelines incorporate the sloshing wave height, the hydrodynamic pressure the contained fluid exerts on the tank wall, the shear forces and moments at the base. Moreover, the solutions adopted in the design guidelines are based on simplified methods with a number of restrictions. The fluid is assumed to be inviscid, incompressible, and have constant density. Although the methodologies are developed mostly for tanks fully filled with liquid, two important phenomena are commonly ignored: the spillage if the top of the tank is open, and the sloshing impact on the roof if the tank is covered.

A thorough understanding of the sloshing impact is needed to determine the safety of the tanks currently in existence in tank farms, and to develop guidelines for enhanced safety in future designs.

There are a very limited number of studies in the field of sloshing impact. Kobayashi (1980) is one of the earlier works on the effects of impulsive pressure due to sloshing impact. Minowa (1980) reported his test results on rectangular tanks. A more recent study by Kurihara, et al. (1992) was focused on experiments, and proposed a simplified formula to predict the impact pressures on the roof.

During the recent tests conducted at the National Research Institute for Earth Science and Disaster Prevention (NIED), severe damage on the steel beam used for the roof deformation sensors was observed (Minowa et al., 1994).

The present study is concerned with the development of a computational formulation to simulate the sloshing impact in roofed tanks. In modeling fluid impact, the choice of pressures computed from instantaneous velocities was used by Wang (1978). A similar approach is adopted in this work. The formulation is incorporated into the in-house finite element computer code FLUSTR-ANL in conjunction with the existing pressure-velocity fluid element. Simulations are performed for a typical storage tank subjected to a resonant harmonic input ground motion. The fluid is allowed to hit the roof on both sides of the tank to study the effect of repeated roof impacts. The results are presented in terms of a series of snapshots of the mesh at some selected times, and time-history plots of the displacements and velocities of some important surface nodes. The dynamic pressure induced in some surface elements is analyzed to determine the effect of the impact on the overall response. The impacting surface nodes and the total contact times/durations are also identified.

DISTRIBUTION OF THIS DOCUMENT IS UNLIMITED

MASTER

DISCLAIMER

Portions of this document may be illegible in electronic image products. Images are produced from the best available original document.

ANALYSIS

Formulation of Liquid Sloshing Impact

The behavior of a Newtonian, isothermal, compressible, viscid fluid is governed by the continuity and momentum equations given in Cartesian coordinate system

$$\frac{1}{\beta} p_{,t} + v_{k,k} = 0 \tag{1}$$

and

$$\rho\left(v_{i,t} + v_{i,j}v_j\right) = -p_{,i} + \mu\left(v_{i,j} + v_{j,i}\right)_{,j} + b_i \tag{2}$$

where β is the bulk modulus, ρ is the mass density, μ is the dynamic viscosity, v_i is the velocity component, p is the pressure, and b_i is the body force component. The subscript t denotes the time derivative, the subscripted indices refer to spatial derivatives, and repeated indices indicate summation.

After imposing the appropriate boundary and initial conditions, the weak forms of Eqs. (1) and (2) can be obtained

$$\int_\Omega \frac{1}{\beta} \delta p p_{,t} d\Omega + \int_\Omega \delta p v_{k,k} d\Omega = 0 \tag{3}$$

and

$$\int_\Omega \rho \delta v_i v_{i,t} d\Omega + \int_\Omega \rho \delta v_i v_{i,j} v_j d\Omega = \int_\Omega \delta v_{j,j} p d\Omega - \int_\Omega 2\mu \delta v_{(i,j)} v_{(i,j)} + \int_\Omega \delta v_i b_i d\Omega + \int_\Gamma \delta v_i h_i d\Gamma + \int_\Gamma \delta v_i h_i^{im} d\Gamma \tag{4}$$

where Ω and Γ denote the domain and the boundaries, respectively. The last term in Eq. (4) represents the effect of liquid impact on the boundary. For the liquid sloshing problem, the surface traction, h_i, is determined from the free surface displacements:

$$h_1 = h_2 = 0 \qquad h_3 = \rho g \eta \tag{5}$$

where g and η are the gravitational acceleration and the free surface displacement, respectively.

Sloshing impact can be modeled by a one-dimensional pressure force, as indicated in Eq. (4). Similar to Eq. (5), the surface traction can be decomposed into its components

$$h_1^{im} = h_2^{im} = 0 \qquad h_3^{im} = \rho c v_3 \tag{6}$$

where c is the velocity of sound in the fluid, and v_3 denotes the velocity at the time of impact.

Finite Element Formulation

The matrix governing equations are derived using a Lagrangian formulation. One pressure node per element is chosen, and the velocity field is given by

$$v_i = \sum_{I=1}^{nen} N_{Ii} v_{iI} \qquad i = 1, nsd$$

where N_{Ii} and v_{iI} are the finite element shape functions and nodal velocities, respectively; nen and nsd denote the number of nodes per element and the number of space dimensions, respectively.

The spatially discretized forms of the weak forms introduced in Eqs. (3) and (4) are given as

$$\mathbf{M^p \dot{p} + G^T v = 0} \tag{7}$$

and

$$\mathbf{M^F \dot{v} + K_\mu v - G p = f} \tag{8}$$

where a superposed "T" denotes the transpose of a matrix, and

$$\mathbf{M^p} = \int_\Omega \frac{1}{\beta} d\Omega$$

$$\mathbf{G^T} = \int_\Omega \mathbf{N_{k,k}} d\Omega$$

$$\mathbf{M^F} = \int_\Omega \rho \mathbf{N^T N} d\Omega$$

$$\mathbf{K_\mu} = \int_\Omega 2\mu \mathbf{N_{,j}^T N_{,j}} d\Omega$$

$$\mathbf{f} = \int_\Omega \mathbf{N^T b} d\Omega + \int_\Gamma \mathbf{N^T h} d\Gamma + \int_\Gamma \mathbf{N^T h^{imp}} d\Gamma$$

Impact Algorithm

In order to capture the impact phenomenon, the vertical displacement of the surface nodes have to be compared to the input gap distance. If the displacement of a node exceeds the allowed value, an appropriate restoring force needs to be computed. This force is treated similar to the free surface pressure. Since there is only one pressure node per element, the surface velocity field has to be used to obtain the impact pressure. The total traction force due to the impact is then formed and added into the global force vector for solution.

This approach is based on the instantaneous velocity at the time of impact, and, hence, requires small time steps to avoid inaccurate results and/or numerical instabilities. The cause of inaccuracy and instability can be explained as follows:

(i) The detection of impact is based on a comparison of surface nodal displacements with prescribed allowable values. Therefore, an overshoot in displacements is necessary to

compute the restoring force. The choice of small time steps is the only way to keep this continual overshooting under control.

(ii) If the overshoot is large (due to a large time step), a large restoring force will be computed. An onset of numerical instability is very likely.

(iii) The restoring force at t_{n+1} is computed from the velocity field at t_n. This approach may induce an oscillatory response.

A summary is presented below:

- Loop over surface nodes for time t_{n+1}
- Check impact: $d_3 > \bar{d}$ $\bar{d}$: initial gap
  d_3: vertical displacement at t_n
- Compute the impact pressure: $p_{im} = \rho c v_3$

  where the velocity field is determined from the nodal velocities (at t_n)

$$v_3 = \sum_{I=1}^{nens} N_{3I} v_{3I}$$

  nens: number of nodes on the surface element

- Form the restoring force

$$f_J = \int_\Gamma N_J p_{im} d\Gamma$$

- Add to the global force vector
- Solve for the response at time t_{n+1}
- Proceed to t_{n+2}

This formulation is incorporated into the in-house computer code FLUSTR-ANL.

RESULTS AND DISCUSSION

The response of a rigid tank with a rigid roof is simulated using the modified in-house computer code FLUSTR-ANL. The FLUSTR-ANL is an implicit finite element code that includes various element libraries. The sloshing impact formulation is added to the fluid finite element which uses both the nodal velocities and the element pressure to model the fluid behavior under seismic motion. The element can successfully handle slightly compressible and viscous fluids.

The tank used in numerical tests has a diameter of 2.4 m (94.5 in.), a total height of 2 m (78.74 in.), and is filled at 90% of its height with water. The finite element mesh is a half model of the tank with 660 fluid elements. Since the roof is assumed to be flat, the same initial gap size of 0.2 m (7.874 in.) is assigned to all surface nodes. The mesh and the node/element numbering are given in Fig. 1.

The response of this tank is studied under a harmonic excitation with an input frequency near the first sloshing frequency (0.5 Hz). Due to relatively large number of steps required to avoid numerical instabilities and severe degradation in accuracy, the response is simulated for the first four seconds of the excitation. This duration is enough to observe impact on either side of the tank. Snapshots at selected times are presented in Figs. 2. Figures 2a-c represent fluid sloshing with vertical displacements not large enough to cause impact on the roof. The surface of the fluid implies linear sloshing behavior. Figure 2d is a snapshot right before the first impact (t = 2.54 sec). The impact of several nodes is observed in Fig. 2e (t = 2.61 sec). Figure 2f depicts the mesh when some of the impacting nodes start separating from the roof (t = 2.66 sec). The opposite end of the tank experiences impact after t = 3.37 sec, as depicted in Fig. 2g. Figure 2h shows the instance when a few nodes are in contact with the roof, and when the fluid has started separating from the roof (t = 3.47 sec). The total separation from the roof is represented by Fig. 2i (t = 3.87 sec).

For a better understanding of the impact phenomenon, the time-history of the displacements, velocities at two nodes (105 and 129), and the pressures in two elements (1 and 12) at the opposing ends of the tank are presented (see Fig. 1). The time-history of the displacements at node 105 is depicted in Fig. 3. The first impact occurs at approximately 2.54 seconds into the excitation at node 131. The impact at node 105 is observed after about 0.03 seconds. The velocity of node 105 is decreased slightly when node 131 first comes in contact with the roof (Fig.4). The expected drop to zero at node 105 occurs at the actual time of contact. Each sharp peak seen in the velocity time-history represents an impact of a different node on the roof. Due to the slightly compressible nature of water, the waves induced by the impact at one node propagate through the mesh affecting the response of other nodes. Each impact is followed by a period of nearly zero velocities implying a continuing contact with the roof. The high-frequency oscillations observed in this period are believed to be mostly numerical, and have very small amplitudes.

The identification of impacting nodes is easier on the pressure time-history of element 1. As it is the case with the velocity time-history, each sharp peak, as seen in Fig. 5, indicates the hit of a node on the roof. The time-history of element 1 has more than four sharp peaks (the number of surface nodes it owns). Again, this indicates that an impact wave has propagated through the mesh and has an immediate and significant effect on the other elements. The main difference from the velocity time-history (Fig. 4) is the fact that the oscillations between two peaks are heavier for the pressure time-history. This is attributed to the finite element formulation of the fluid which is represented by eight velocity nodes and only one pressure node per element. In summary, a total of 7 nodes in the following order impact with the roof: 131, 105, 107, 132, 144, 145, and 133. Three elements are in full and one element in partial contact with the roof. At about 2.66 seconds, all the nodes separate from the roof, and the fluid starts swinging to the opposite end. The total impact time is approximately 0.12 seconds.

In order to study the effects of repeated impact on the fluid behavior, the computations are continued at approximately 3.37 seconds into the excitation, node 143 hits the roof at the opposite end. The impact characteristics are the same as the other end of the tank as indicated earlier. The time-history of the displacement, and the velocity of the node 129 are presented in Figs. 6 and 7, respectively. The pressure time-history of element 12 which also includes node 129 is given in Fig. 8.

Since the input excitation used in this example is near the first sloshing frequency of the tank (near resonance), and no damping (artificial or viscosity-based) is applied, the response is expected to grow with time. Consequently, the impact on this side of the tank is larger in amplitude and lasts longer, approximately 0.47 seconds, ending at time equal to 3.84 seconds.

Fifteen (15) nodes come in contact with the roof in the following order: 143, 129, 127, 142, 156, 155, 141, 125, 154, 168, 169, 140, 123, 167, and 182. The mesh distortion on the fluid surface becomes apparent after the second impact whereas no significant surface distortion can be observed for the first impact.

CONCLUSIONS

An impact formulation based on pressure induced by the instantaneous velocity at the instance of impact is derived. The formulation is incorporated into the pressure-velocity element already in existent in the in-house computer code FLUSTR-ANL. An example case with geometrical dimensions of a typical HLW storage tank is analyzed under resonant harmonic excitation. The simulation results are presented in terms of snapshots of the finite element mesh at selected instances, and in terms of time-history plots of the surface displacements, velocities of selected nodes, and the pressures of selected elements. The fluid is allowed to hit the roof on either side of the tank to study the impact characteristics. No significant changes can be detected on the fluid surface following the first impact. The fluid retained a behavior similar to the linear response preceding the impact. Due to the relatively larger surface displacements, more nodes come in contact with the roof on the second impact sequence inducing some surface distortion. The time-history plots provide useful information about important characteristics such as surface displacements staying constant, velocities diminishing to near zero values during the impact, and element pressures with large peaks indicating the onset of impact.

The next step in validating the formulation is a comparison with some relevant experiments performed on sloshing impact in roofed tanks.

ACKNOWLEDGMENT

Work performed under the auspices of the U.S. Department of Energy under Contract W-31-109-Eng-38.

REFERENCES

Kobayashi, N., 1980, "Impulsive Acting on the Tank Roofs Caused by Sloshing Liquid," *Proceedings, 7th World Conference on Earthquake Engineering*, Vol. 5, pp. 315-322.

Kurihara, C., Masuko, Y., and Sakurai, A., 1992, "Sloshing Impact Pressure in Roofed Liquid Tanks," *ASME Pressure Vessel and Piping Conference*, New Orleans, LA, PVP-Vol. 232, pp. 19-24.

Minowa, C., Ogawa, N., Harada, I., and Ma, D. C. 1994, "Sloshing Roof Impact Tests of a Rectangular Tank," 1994 *ASME Pressure Vessel and Piping Conference*, Minneapolis, MN, PVP-Vol. 272, pp. 13-21.

Minowa, C., 1980, "Dynamic Analysis for Rectangular Water Tanks," *ASME Pressure Vessel and Piping Conference*, PVP-Vol. 43, pp. 135-141.

Wang, C. Y., 1978, "Comparison of ICECO Code Predictions with Flexible Vessel Experiments," *Nuclear Engineering and Design*, Vol. 49, pp. 145-154.

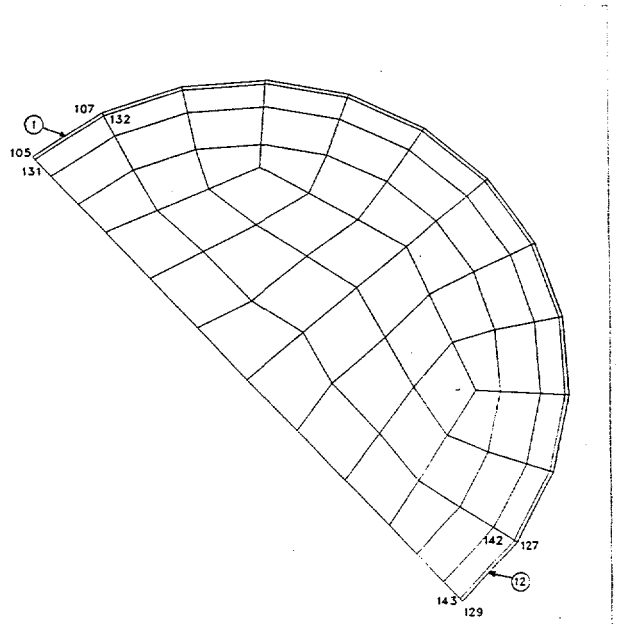

FIG. 1. FLUID SURFACE AND NODE/ELEMENT NUMBERING

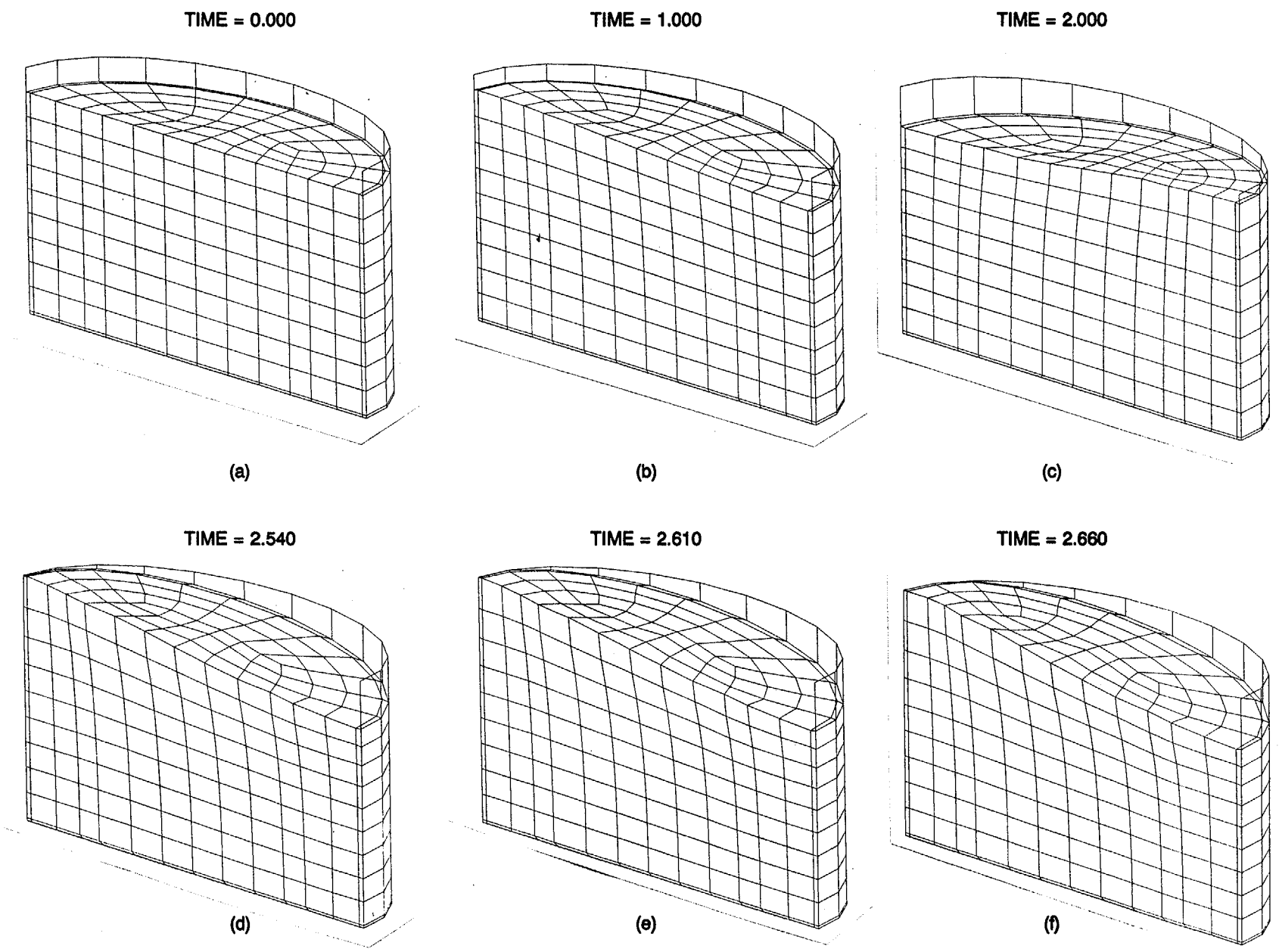

FIGS. 2. MESH SNAPSHOTS AT SEVERAL INSTANCES DURING EXCITATION

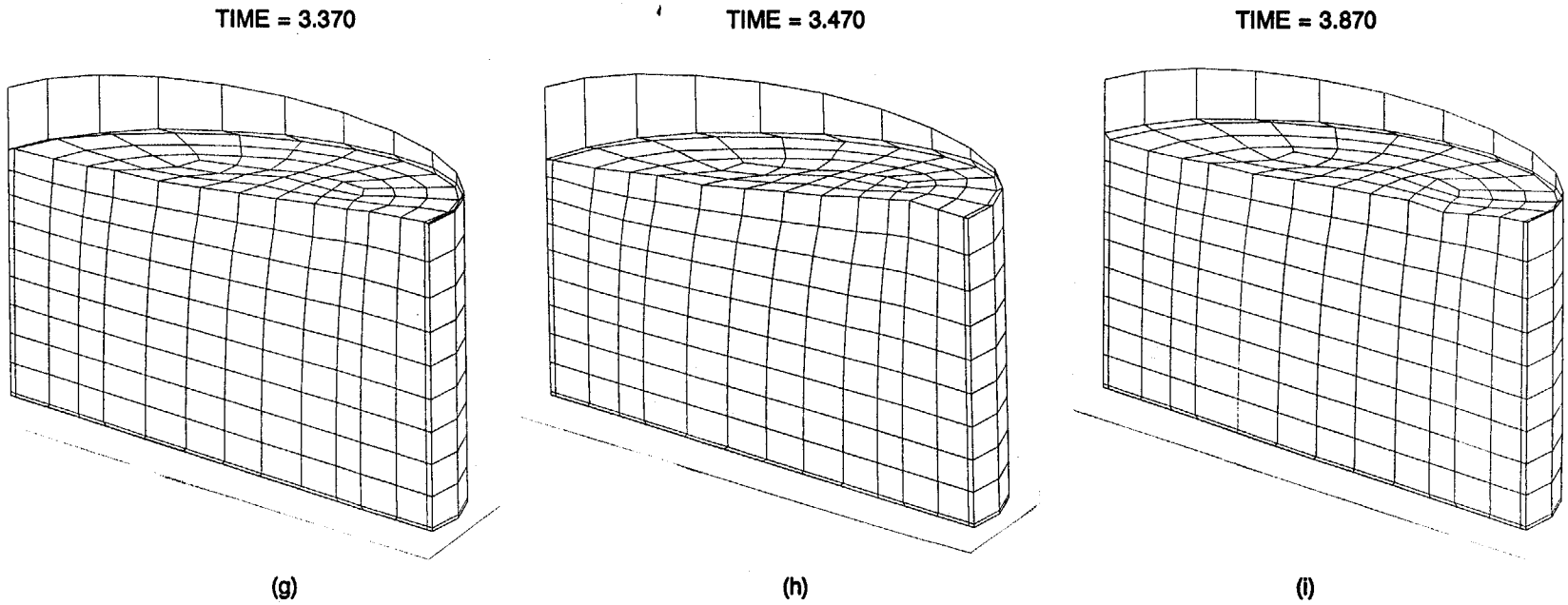

FIGS. 2. MESH SNAPSHOTS AT SEVERAL INSTANCES DURING EXCITATION (Continued)

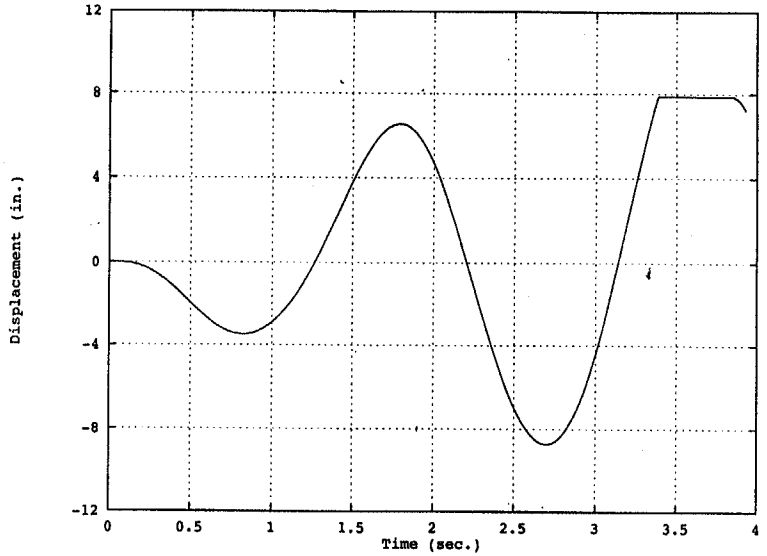

FIG. 6. DISPLACEMENT TIME-HISTORY FOR NODE 129

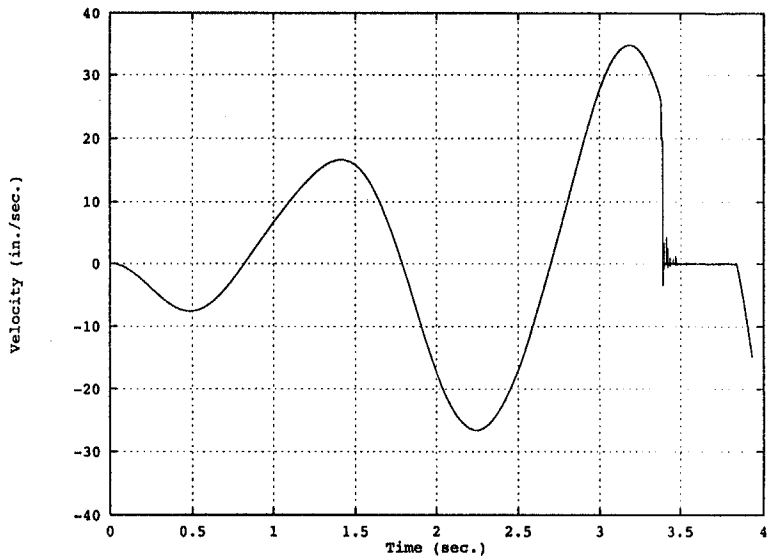

FIG. 7. VELOCITY TIME-HISTORY FOR NODE 129

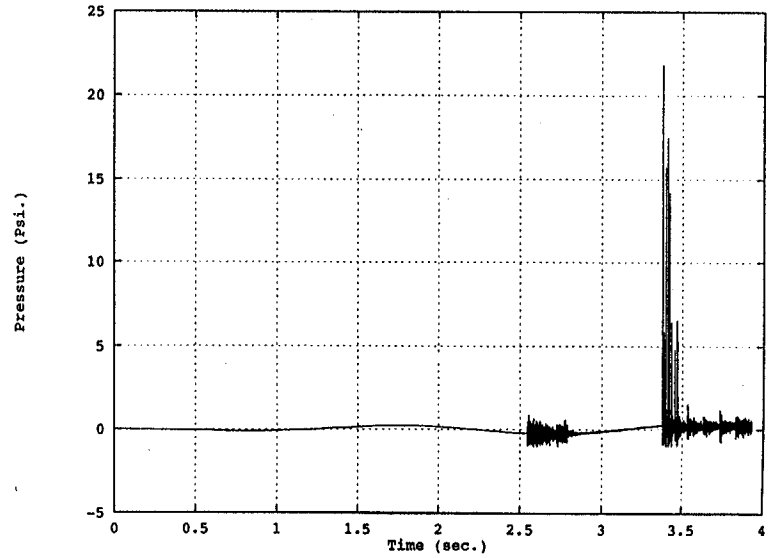

FIG. 8. PRESSURE TIME-HISTORY FOR ELEMENT 12

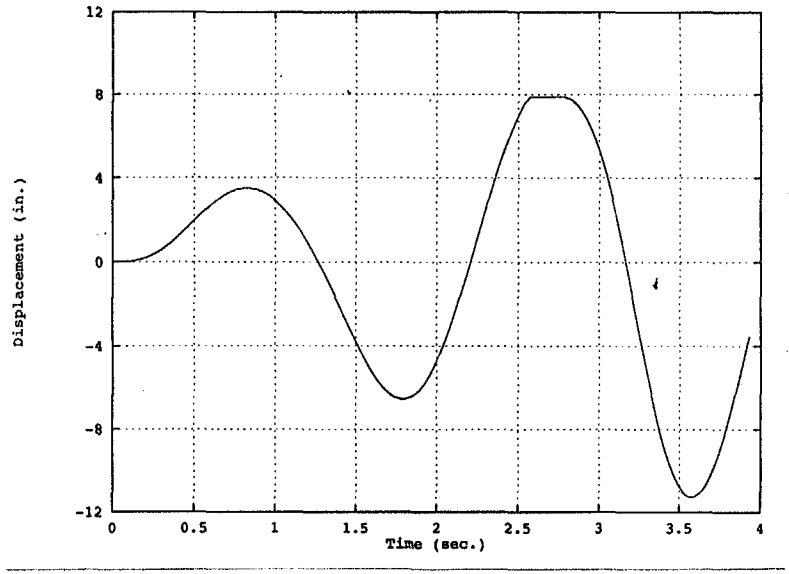

FIG. 3. DISPLACEMENT TIME-HISTORY FOR NODE 105

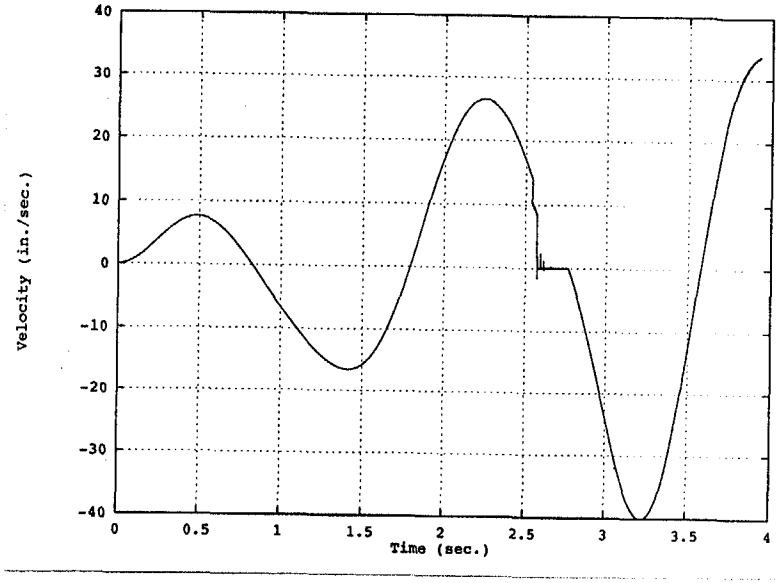

FIG. 4. VELOCITY TIME-HISTORY FOR NODE 105

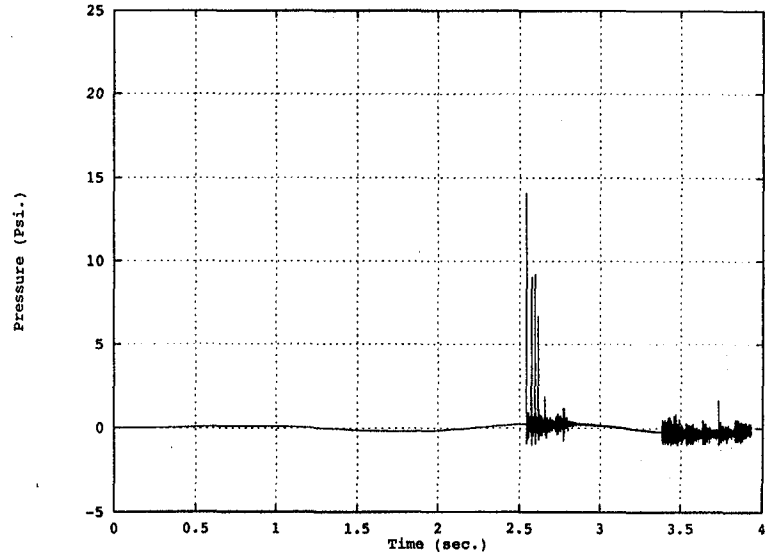

FIG. 5. PRESSURE TIME-HISTORY FOR ELEMENT 1